THE JOURNAL OF BIOLOGICAL CHEMISTRY VOL. 289, NO. 14, pp. 9547–9559, April 4, 2014

Loss of Syndecan-1 Induces a Pro-inflammatory Phenotype in Endothelial Cells with a Dysregulated Response to Atheroprotective Flow*[S]

Received for publication, December 10, 2013, and in revised form, February 11, 2014 Published, JBC Papers in Press, February 19, 2014, DOI 10.1074/jbc.M113.541573

Peter L. Voyvodic[‡], Daniel Min[‡], Robert Liu[‡], Evan Williams[‡], Vipul Chitalia[§], Andrew K. Dunn[‡], and Aaron B. Baker[‡1]

From the [‡]Department of Biomedical Engineering, University of Texas at Austin, Austin, Texas 78712 and the [§]Renal Section, Department of Medicine, Boston Medical Center, Boston University School of Medicine, Boston, Massachusetts 02118

Background: The endothelial glycocalyx extends into the arterial lumen and experiences shear forces from blood flow.
Results: The loss of syndecan-1 results in a pro-inflammatory phenotype in endothelial cells with an altered response to atheroprotective flow.
Conclusion: Syndecan-1 plays an important role in maintaining healthy endothelial phenotype.
Significance: Therapies that retain syndecan-1 on endothelial cells may have the potential to reduce the progression of vascular disease.

Fluid shear stresses are potent regulators of vascular homeostasis and powerful determinants of vascular disease progression. The glycocalyx is a layer of glycoaminoglycans, proteoglycans, and glycoproteins that lines the luminal surface of arteries. The glycocalyx interacts directly with hemodynamic forces from blood flow and, consequently, is a prime candidate for the mechanosensing of fluidic shear stresses. Here, we investigated the role of the glycocalyx component syndecan-1 (sdc-1) in controlling the shear stress-induced signaling and flow-mediated phenotypic modulation in endothelial cells. We found that knock-out of sdc-1 abolished several key early signaling events of endothelial cells in response to shear stress including the phosphorylation of Akt, the formation of a spatial gradient in paxillin phosphorylation, and the activation of RhoA. After exposure to atheroprotective flow, we found that sdc-1 knock-out endothelial cells had a phenotypic shift to an inflammatory/pro-atherosclerotic phenotype in contrast to the atheroprotective phenotype of wild type cells. Consistent with these findings, we found increased leukocyte adhesion to sdc-1 knock-out endothelial cells *in vitro* that was reduced by re-expression of sdc-1. *In vivo*, we found increased leukocyte recruitment and vascular permeability/inflammation in sdc-1 knock-out mice. Taken together, our studies support a key role for sdc-1 in endothelial mechanosensing and regulation of endothelial phenotype.

Arterial mechanotransduction has been the subject of intense experimental and theoretical study over the past decades (1, 2). The search for potential mechanotransducers, molecules that serve as force sensors and activators of mechanical responses, has revealed a variety of intricate mechanisms through which hemodynamic forces can alter arterial biology (3–7). A key finding in these studies is that certain arterial flow profiles induce an atheroprotective phenotype in endothelial cells leading to broad alterations in endothelial function relating to inflammation, vasodilation, and thrombosis, whereas other profiles induce a more inflammatory, atheroprone phenotype (2). Multiple signaling and transcriptional regulators, such as the Krüppel-like factor (KLF)[2] family of transcription factors, have been found to strongly modulate this response (8–11). Several key mechanosensitive elements have been identified in endothelial cells, including platelet endothelial cell adhesion molecule (PECAM-1), cadherins, and the actin cytoskeleton (12), but the full scope and complexity of the mechanosensing mechanisms remains unclear.

The endothelial glycocalyx is a structure of glycans and proteoglycans present on the luminal surface of arteries. Recent cryo-electron microscopy images have shown that it can extend up to 11 μm into the lumen, inevitably making it the endothelial structure first exposed to changes in fluid shear stress (13). In addition, modeling studies have postulated that the entirety of fluid shear force is dissipated in the glycocalyx before reaching the cell membrane (14). Removal of heparan sulfate glycoaminoglycans from the cell surface using enzymatic digestion reduces endothelial production of vasodilatory factors in response to shear stress (15). However, it is unknown which proteoglycans are important in these processes, as well as their scope of mechanistic involvement in mechanosensing of shear stress.

The syndecan family of transmembrane cell surface proteoglycans are an appealing group of candidate molecules for mechanosensing because of their location at the cell surface and interactions with integrins and cytoskeletal elements (16). The syndecans are single-pass transmembrane proteins known to be capable of transmitting extracellular signals into intracellular signaling pathways (17). These molecules are a component

* This work was supported, in whole or in part, by National Institutes of Health Director's New Innovator Grant DP2 OD008716-01 (to A. B. B.). This work was also supported by American Heart Association Grant 10SDG2630139.
[S] This article contains supplemental Videos S1–S3.
[1] To whom correspondence should be addressed: University of Texas at Austin, Dept. of Biomedical Engineering, 107 West Dean Keeton St., BME 5.202D, C0800, Austin, TX 78712. Tel.: 512-232-7114; E-mail: abbaker1@gmail.com.

[2] The abbreviations used are: KLF, Krüppel-like factor; sdc, syndecan; S1KO, sdc-1 knock-out.

of the glycocalyx and are likely exposed to extracellular forces from flow and adherence to the extracellular matrix. In addition, the cytoplasmic domain of syndecans interact with cytoskeletal and focal adhesion complex proteins as well as multiple intracellular signaling pathways (18). The syndecans act synergistically with integrins through their extracellular domain and serve as regulators of cell adhesion (19–21). Thus, syndecans and other cell surface proteoglycans are uniquely positioned to interact with externally applied mechanical forces and transmit these signals to multiple pathways within the cell.

Here, we hypothesized that syndecan-1 (sdc-1) is a critical element in shear stress-mediated signaling and phenotypic regulation in endothelial cells. Using endothelial cells isolated from sdc-1 knock-out mice, we demonstrate that sdc-1 is required for the activation of Akt and RhoA and for the formation of a phosphorylation gradient in paxillin in the initial stages of the endothelial response to shear stress. In addition, sdc-1 knock-out profoundly alters the shear stress-induced expression of transcription factors, vasodilatory mediators, and inflammatory soluble factors and receptors. Based on these findings, we propose that sdc-1 is an important atheroprotective molecule that governs both the inflammatory state of the endothelial cells and the induction of atheroprotective phenotypes by shear stress. Thus, this work expands our limited understanding of the role of cell surface proteoglycans in vascular mechanobiology and may provide insight into the mechanisms of shear stress-mediated regulation of atherogenesis.

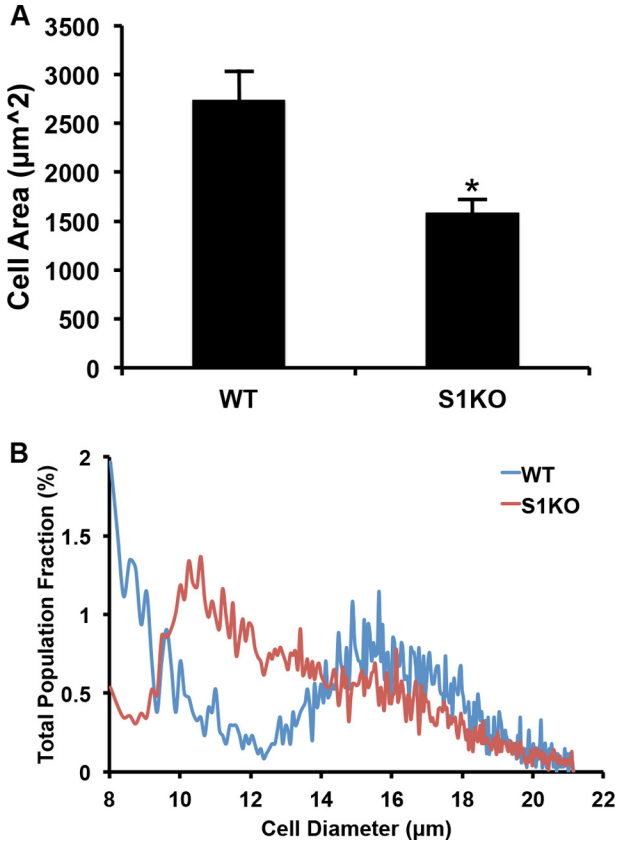

FIGURE 1. **Loss of sdc-1 results in reduced cell size and adhesion area.** *A*, S1KO endothelial cells adhered to a smaller surface area than the WT cells ($n > 40$). *, $p < 0.05$ for S1KO *versus* WT group. *B*, the volume of S1KO cells is reduced compared with the WT model.

EXPERIMENTAL PROCEDURES

Cell Culture—Endothelial cells were isolated from the lungs of wild type and syndecan-1 knock-out mice as previously described (22). Briefly, the lungs were macerated and digested with collagenase followed by sorting with CD31 Dynabeads (Invitrogen). After cells were expanded, they underwent a second round of CD31 Dynabead sorting to ensure cell purity. Endothelial phenotype was confirmed using cellular uptake of fluorescently labeled Ac-LDL and through the expression of Tie-2 mRNA. Cells were later examined for size differences caused by the loss of sdc-1 (Fig. 1). Area was calculated using Metamorph software (Molecular Devices) with over 20 cells for both wild type and sdc-1 knock-out cells. Volume was measured using a Z-series Coulter counter (Beckman Coulter). We also measured gene expression to evaluate compensatory increases in other heparan sulfate proteoglycan core proteins and synthetic enzymes (Fig. 2). The cells were cultured in MCDB-131 media with 5% FBS and antibiotics (Invitrogen).

Cloning of Lentiviral Constructs for Expressing Wild Type and Mutant Forms of Syndecan-1 and Expression in Endothelial Cells—To allow robust expression in primary vascular cell lines, we cloned the sdc-1 gene into an enhanced lentiviral expression system (23) (kind gift of Dr. Gustavo Mostoslavsky, Boston University) and validated the expression of sdc-1 in vascular cells. This lentiviral system is highly efficient in infecting vascular cells and led to over 99% efficiency of cells as measured by constitutive expression of GFP through an internal ribosome entry site promoter incorporated into the vector. The construct was confirmed by DNA sequencing and nuclease digestion. The lentiviral vector was then transfected with packaging vectors into a HEK-293T packaging line to allow viral production and transduced into cells as previously described (23).

In Vitro Flow Studies—For Western lysis flow experiments, cells were seeded onto glass slides coated with fibronectin; for all other flow experiments, cells were seeded into multichannel flow chambers (μ-Slide $VI^{0.4}$; Ibidi). Flow was applied using a multichannel flow device that provides steady flow in up to 24 flow channels simultaneously as previously described (24). The entire system was kept in an incubator at 37 °C with a 5% CO_2 atmosphere throughout the experiment.

Immunocytochemical Staining—Following treatments, the cells were washed with PBS and fixed in 4% paraformaldehyde for 20 min. The cells were quenched with 0.2 M glycine and then permeabilized with 0.2% Triton X-100 and blocked with 5% FBS in PBS, 1% BSA for 1 h. Next, the cells were labeled with a 1:100 dilution of primary antibodies in PBS, 1% BSA overnight at 4 °C. They were then washed three times in PBS, 1% BSA and labeled with a 1:1000 dilution of fluorescently labeled secondary antibody for 1 h at room temperature. For experiments studying the actin cytoskeleton, the cells were also labeled with a 1:500 dilution of Alexa 594-labeled phalloidin (Invitrogen) for 1 h at room temperature. Finally, the cells were washed five times in PBS, 1% BSA, mounted in a DAPI-containing mounting medium (Vector Labs), and imaged using an epifluorescent microscope (Carl Zeiss). Morphometric and intensity analysis of the cells was performed using Metamorph software (Molecular Devices) and Photoshop software (Adobe). The following

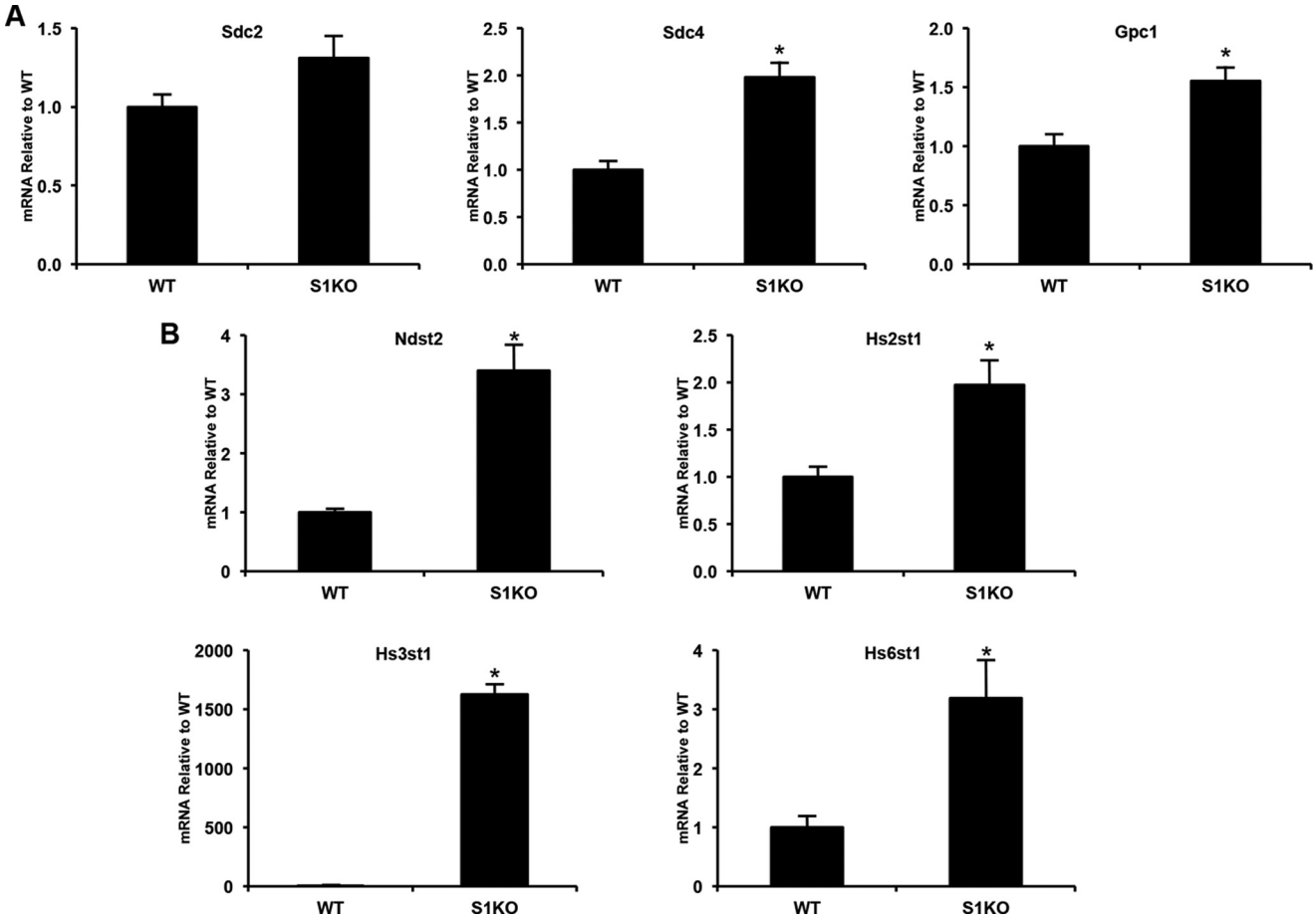

FIGURE 2. **Loss of sdc-1 alters the expression of other glycocalyx components and heparan sulfate sulfotransfereases.** WT and S1KO endothelial cells were lysed under static conditions and examined for gene expression ($n = 6$). *A*, S1KO endothelial cells express higher levels of other glycocalyx components, particularly sdc-4 and gpc-1. *, $p < 0.05$ for S1KO *versus* WT group. *B*, expression of sulfotransferases was dramatically increased in the S1KO model. *, $p < 0.05$ for S1KO *versus* WT group.

antibodies were used for immunostaining: phospho-Akt (Ser^{473}) and Akt from Cell Signaling; phosphopaxillin (Tyr^{118}) from Invitrogen; paxillin from BD Biosciences; and secondary antibodies from Santa Cruz Biotechnology. Activation of integrin $\alpha_v\beta_3$ was detected with the WOW-1 antibody using a 1:5 dilution (kind gift of Dr. Shattil Sanford, UCSD).

Cell Lysis and Immunoblotting—Following treatments, the cells were lysed with 20 mM Tris, 150 mM NaCl buffer (pH 8.0) containing 1% Triton X-100, 0.1% SDS, 2 mM sodium orthovanadate, 2 mM PMSF, 50 mM NaF, and 1 complete protease inhibitor pellet (Roche Applied Science) per 50 ml of lysis buffer. For Western blotting, a 1:500 dilution of primary antibodies (phospho-Akt (Ser^{473}) and Akt from Cell Signaling) was used for overnight incubation at 4 °C, and a 1:3500 dilution of secondary antibodies (Santa Cruz Biotechnology) was used at room temperature for 2 h as previously described (25).

Focal Adhesion Quantification—Fluorescent images were acquired for endothelial cells immunostained for paxillin and phosphorylated paxillin. The images were background-subtracted, and the phosphopaxillin image was divided by the total paxillin image using Photoshop (Adobe). The gray scale image was then indexed and assigned to a linear pseudocolor lookup table with a value of 0 assigned to black to differentiate the cell from the background. Line scans of the gray scale ratio image were generated using Metamorph software.

Colocalization Analysis—Following flow, images were acquired from stainings for actin and a high affinity form of integrin $\alpha_v\beta_3$ using the WOW-1 antibody. Pearson correlation coefficients were calculated for 10 cells in each condition using ImageJ open source software and plug-ins developed by the Bob and John Wright Cell Imaging Facility of the University of Ontario Canada.

Measurement of RhoA Activity Using FRET—The plasmid for the RhoA-FRET Biosensor construct was used as previously described (pBabe-Puro-RhoA Biosensor; Addgene) (26). The plasmid was transfected into packaging HEK293T cells using Lipofectamine 2000 (Invitrogen) to produce retroviruses. Viruses were collected after 48 h, centrifuged to remove cell debris, filtered with a 0.45-μm filter, and added at a 50% final concentration to WT or sdc-1 knock-out endothelial cells. The medium was replaced after 24 h, and the cells were given 48 h to recover before undergoing resistance selection with 1 μg/ml puromycin for 10 days followed by selection with 10 μg/ml puromycin for an additional 10 days. During selection and routine cell culture, the medium contained 10 μg/ml doxycycline to suppress RhoA construct transcription through a TetCMV

TABLE 1

Primers used for real time PCR

KLF, Krüppel-like factor; eNOS, endothelial nitric-oxide synthase; Tie2, tyrosine kinase with immunoglobulin-like and EGF-like domains-2; Ang2, angiopoietin-2; CNP, c-type natriuretic peptide; ET1, endothelin 1; ICAM1, intercellular adhesion molecule 1; VCAM1, vascular cell adhesion protein 1; MCP-1, monocyte chemotactic protein-1; MIP2α, macrophage inflammatory protein 2α; CXCL1, chemokine (*CXC* motif) ligand 1; ASS, argininosuccinate synthase; IP10, interferon γ-induced protein 10; COX2, cytochrome *c* oxidase subunit II; CCL5, chemokine (CC motif) ligand 5; MIP1γ, macrophage inflammatory protein 1γ; SDF1, stromal cell-derived factor-1; Sdc2, syndecan-2; Sdc4, syndecan-4; Gpc1, glypican 1; Ndst2, *N*-deactylase/*N*-sulfotransferase 2; Hs2st1, heparan sulfate 2-*O*-sulfotransferase 1; Hs3st1, heparan sulfate 3-*O*-sulfotransferase 1; Hs6st1, heparan sulfate 6-*O*-sulfotransferase 1.

Gene	Forward primer	Reverse primer
KLF2	TCTGCGTACACACACAGGTGAGA	TGTGCTTTCGGTAGTGGCGGGT
KLF4	CGGGCAATCTGGGGGTTTTGGT	TCGCCAGGTGGCTGCCTCATTA
KLF5	AACCCGGATCTGGAGAAGCGAC	ACTTGTAGGGCTTCTCGCCCGT
eNOS	TGAGGTCAGCTGGCATGGGCAA	TGCTTGCCGCACAGCCCTAA
Tie2	AGCCGCACACATTTGGCAGGA	TGTGGCACAGGAACACCCGT
Ang2	ATGGCGATGAGCCCAGGTCCTT	TCGTCCCGGCCTTTTGGCTT
CNP	TGCTCGCTTGGCAATCCTGCT	TCAGCTGGGAGAGGTGCATGGT
ET1	TCTGGCTGCACGTTGCCTGT	GGACAGTTCTCCGCCGCCTTTT
ICAM1	TTCAACCCGTGCCAAGCCCA	AGTTCACCTGCACGGACCCA
VCAM1	TGGCTCTGGGAAGCTGGAACGA	ACACTTGACCGTGACCGGCT
E-selectin	TGAGCTGCAGCCACTCAACAGC	TGCGCTGCATTCAACCTGCG
MCP-1	AGCACCAGCACCAGCCAACTCT	AGCCGGCAACTGTGAACAGCA
CXCL2	AGCCACTCTCAAGGGCGGTCAA	TCTTCCGTTGAGGGACAGCAGC
CXCL1	TCGCCAATGAGCTGCGCTGT	AAGGCAAGCCTCGCGACCAT
Elastin	AGCCAAGTATGGTGCTGGGGGA	TTCCAGCGCCTGCAATGCCT
ASS	TGCCAAAGCACCCAACAGCC	TCCGTGCTTGCCCGCAACTT
IL6	GCTGGAGTCACAGAAGGAGTGGCT	GGCATAACGCACTAGGTTTGCCG
IP10	CCATGAACCCAAGTGCTGCCGT	ATGCAGTTGCAGCGGACCGT
COX2	ACGTGCAACACCTGAGCGGT	TGTTGAAGGTGTCGGGCAGCA
CCL5	TGCCGCGGGTACCATGAAGA	GCAAAGCAGCAGGGAGTGGTGT
IL1α	TCGTCGGGAGGAGACGACTCTA	TCAGCAACACGGGCTGGTCT
IL15	TTACGCGCTGCAGGGACCTT	AGCTGTTAGATGTGGAACTCAGCCT
MIP1γ	GGTGTGAACTGCCAGCTACT	GCTTCAGACCTTCCAGGCAT
SDF1	GGTGCTCAAACCTGACGGTA	GGCAGCTCCTCTTTGGCTTA
Sdc2	CCAGAAGGCACCCACTAAGG	AGGGCCAGTATGGCTCTGTA
Sdc4	AATACAGTGGCCTCGTGTGG	AACCAGCTTAACCCTCGGTG
Gpc1	TAAGGGCTTTAGCCTGAGCG	GCTGTGGTTGGCCAAATTCT
Ndst2	CTTATCCCAGGTCCCGGTCA	TCAAGTACCGCTCCCACCA
Hs2st1	TATGTCTTGATCGCGAGCGG	TGCCTTGCAATTGCCCTTTC
Hs3st1	CGGGGTGAGTGTGAATTTGC	TGAAGTAGCAGCAAGGCTCC
Hs6st1	TCATCCTTTACCAGTACGCGG	TGTGCAGGAAGACGATCACG
GAPDH	CCCCAGCAAGGACACTGAGCAA	GCTCCCTAGGCCCCTCCTGTTATT

repressor. At 48 h prior to the experiment, the cells were given medium without doxycycline to allow for RhoA construct transcription. The cells were seeded in flow chambers (μ-Slide VI$^{0.4}$; Ibidi) and grown to confluence. Using a syringe pump (Kent Scientific), medium was flowed over the cells until the given time points, at which point the channel was immediately read using a plate reader (Varioskan; Thermo-Scientific). To prevent alterations in RhoA activation caused by starting and stopping flow, separate flow channels were used for each time point. The FRET ratio was calculated by dividing the FRET signal (excitation, 436 $\pm$ 12 nm; emission, 535 $\pm$ 12 nm) by the donor signal (excitation, 436 $\pm$ 12 nm; emission, 470 $\pm$ 12 nm) and then normalizing to the acceptor signal (excitation, 500 $\pm$ 12 nm; emission, 535 $\pm$ 12 nm) to account for changes in copy number.

Measurement of Gene Expression by Real Time PCR—Messenger RNA was harvested from the cells following flow using an RNAeasy kit (Qiagen), and the relative mRNA copy numbers were quantified using real time PCR as described previously (27, 28). Copy numbers were normalized to GAPDH gene expression. Forward and reverse primers for each target were as shown in Table 1.

Assay for Monocyte Adhesion—Confluent monolayers of WT, S1KO, and pSyn-1 endothelial cells were grown in slide-mounted flow chambers (Ibidi) and then stimulated with the addition of 10 ng/ml TNF-α for 4 h. The flow chambers were positioned on a inverted microscope, and CellTracker dye (Invitrogen)-labeled THP-1 cells (5×10^5 cells/ml) were perfused through the chamber with a syringe pump (Kent Scientific) for 5 min at a controlled flow rate to generate a shear stress of 0.5 dynes/cm^2. The entire period of perfusion was recorded as a digital video and analyzed to determine the number of rolling THP-1 cells over monolayers in three 90-s intervals. After 5 min the flow was changed to MCDB-131 medium to wash out unadhered cells, and the plates were imaged in eight separate locations. The number of cells adhered per field of view was by quantified using Metamorph software.

Animal Experiments—All animal procedures were conducted in accordance with protocols approved by the University of Texas at Austin's Institutional Animal Care and Use Committee. Syndecan-1 knock-out (Sdc1$^{-/-}$) mice were used as previous described (29) and were a kind gift from Dr. Ram Sasisekharan (Massachusetts Institute of Technology). To examine the inflammatory response of WT and S1KO mice, we anesthetized the mice and applied 5% allyl isothiocyanate, a potent inflammatory/permeability stimulus, to the hind feet of the mice. We subsequently imaged the feet of the mice over time using a laser speckle imager. Laser speckle imaging allows the real time measurement of tissue perfusion with tens of microns spatial and millisecond temporal resolution (30). Briefly, a diode laser (785 nm, 50 milliwatt; Thor Labs) was shown upon the footpad of a mouse hindlimb. A Basler 1920 $\times$ 1080 monochrome CCD with a zoom lens (Zoom7000; Navitar) mounted on a microscope boom stand was placed vertically

over the foot and used to record speckle images of blood perfusion. The raw speckle images were converted into speckle contrast images using the following relation,

$$K = \frac{\sigma_s}{\langle I \rangle} \quad \text{(Eq. 1)}$$

where σ_s is the standard deviation and $\langle I \rangle$ is the mean intensity over a 7 × 7-pixel region of the image. The speckle contrast images were quantified by assigning values of 0, 1, and 2 to the red, green, and blue channels and multiplying by the area to integrate the total signal. Each time point was then normalized to the pre-oil measurement.

Thioglycolate Injection and Detection of CD14-positive Cells—sdc-1 knock-out and wild type mice were given an intraperitoneal injection of 1.5 ml of Brewer thioglycollate medium. After 4 days, the recruited cells were harvested by intraperitoneal lavage. The cells were then fixed and stained using a FITC-labeled antibody for CD14 (BD Biosciences). The cells were then analyzed via FACS analysis using a FACSCalibur sorter (BD Biosciences).

Histological Analysis—The feet of mice from the mustard oil laser speckle experiment were fixed in 4% paraformaldehyde and stored at 4 °C. The foot pads were then removed and stored in PBS, 20% sucrose for 48 h at 4 °C with shaking before freezing in liquid nitrogen cooled isopentane. The frozen foot pads were cryosectioned and stained as described previously (28).

Statistical Analysis—All results are shown as means ± S.E. Comparisons between groups were analyzed using a two-way analysis of variance followed by a Tukey post hoc test. Comparisons between only two groups were analyzed using a Student's *t* test. A two-tailed probability value <0.05 was considered statistically significant.

RESULTS

Loss of Syndecan-1 in Endothelial Cells Inhibits the Activation of Akt in Response to Shear Stress—Shear stress rapidly activates the Akt pathway in endothelial cells leading to alterations in oxidative stress (31), suppression of apoptotic signaling pathways (32), and production of NO (33). We applied shear stress to endothelial cells using a custom *in vitro* system allowing the application of steady flow of culture media through 24 microchannels simultaneously (24). Using this system, WT and sdc-1 knock-out (S1KO) endothelial cells were exposed to 12 dynes/cm^2 of steady shear stress for 15 min. This level of steady shear stress induces an atheroprotective phenotype in endothelial cells that has been well characterized (2). After 5–15 min of exposure to flow, wild type endothelial cells had a robust increase in Akt phosphorylation with an ~2-fold increase in Akt phosphorylation following flow as measured by immunostaining (Fig. 3*A*) and Western blotting (Fig. 3*B*). In contrast, there was minimal activation in sdc-1 knock-out endothelial cells by flow.

Syndecan-1 Knock-out Abrogates the Formation of a Phosphorylation Gradient in Paxillin Following Flow—Endothelial cells are known to modulate their cytoskeletal arrangement and alignment in response to shear stress through the formation of a gradient in paxillin phosphorylation across the cell (34). We

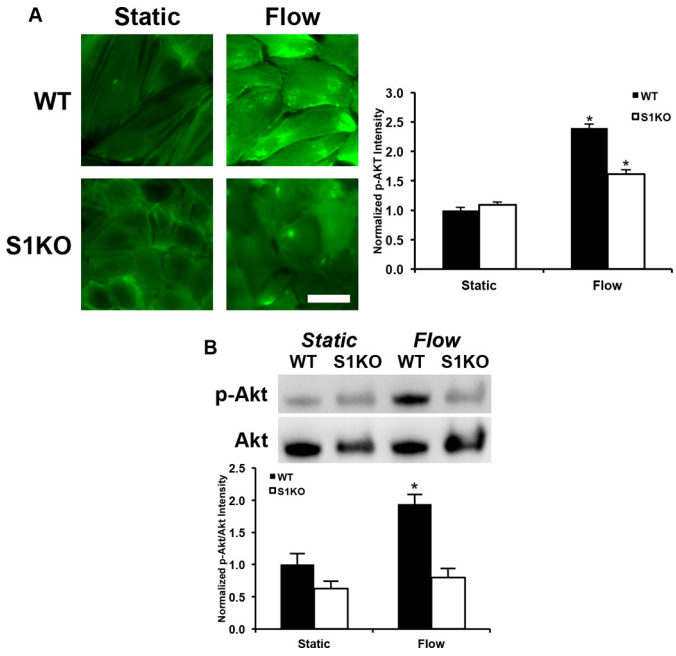

FIGURE 3. **Loss of sdc-1 alters shear stress-induced activation of Akt pathway signaling.** *A*, WT and S1KO were exposed to flow at 12 dynes/cm^2 for 5 min. Immunohistochemical staining demonstrated an increase in Akt phosphorylation (Ser^{473}) in WT cells after flow. In contrast this increase was not observed in the S1KO cells. *Scale bar*, 50 μm. Chart displays semiquantitative analysis of pAkt staining intensity ($n = 40$). *, statistically significant difference *versus* all other groups ($p < 0.05$). *B*, Western blotting analysis of lysed cells following 15 min of flow at 12 dynes/cm^2 revealed a reduced relative phosphorylation of Akt in S1KO cells ($n = 8$). *, statistically significant difference *versus* all ($p < 0.05$).

grew endothelial cells in flow chambers and exposed them to 12 dynes/cm^2 of shear stress for 15 min. We immunostained for paxillin and phosphopaxillin and performed a ratiometric analysis for paxillin phosphorylation from these images. There was a robust formation of a paxillin phosphorylation gradient in the WT cells with higher phosphorylation on the downstream edge of the cell after flow exposure (Fig. 4, *A* and *B*). In contrast, there was no discernable polarity to paxillin phosphorylation for sdc-1 knock-out cells in all cases.

Loss of Syndecan-1 Results in Reduced Colocalization of Activated $\alpha_v\beta_3$ Integrins with the Actin Cytoskeleton under Static and Atheroprotective Flow Conditions—Activation of focal adhesions is an important shear-mediated mechanotransduction pathway and involves accompanying activation of integrins and their association with the actin cytoskeleton (2). Integrin $\alpha_v\beta_3$ is activated by shear stress in endothelial cells adhered to fibronectin or fibrinogen (35) and controls the release of endothelial elastase and FGF-2 in response to flow (36). We exposed confluent endothelial cells to 12 dynes/cm^2 for 5 min and imaged activated integrin $\alpha_v\beta_3$ using the WOW-1 antibody that recognizes the high affinity form of $\alpha_v\beta_3$ (37). Wild type endothelial cells had colocalization between the activated $\alpha_v\beta_3$ integrins and the actin stress fibers, particularly at the periphery of the cell both under static and flow conditions (Fig. 4, *C* and *D*). This colocalization was markedly reduced in sdc-1 knock-out cells under both of these conditions.

Syndecan-1 Knock-out Inhibits RhoA Activation by Shear Stress—Activation of RhoA GTPases is a key step regulating endothelial cytoskeletal remodeling in response to shear stress

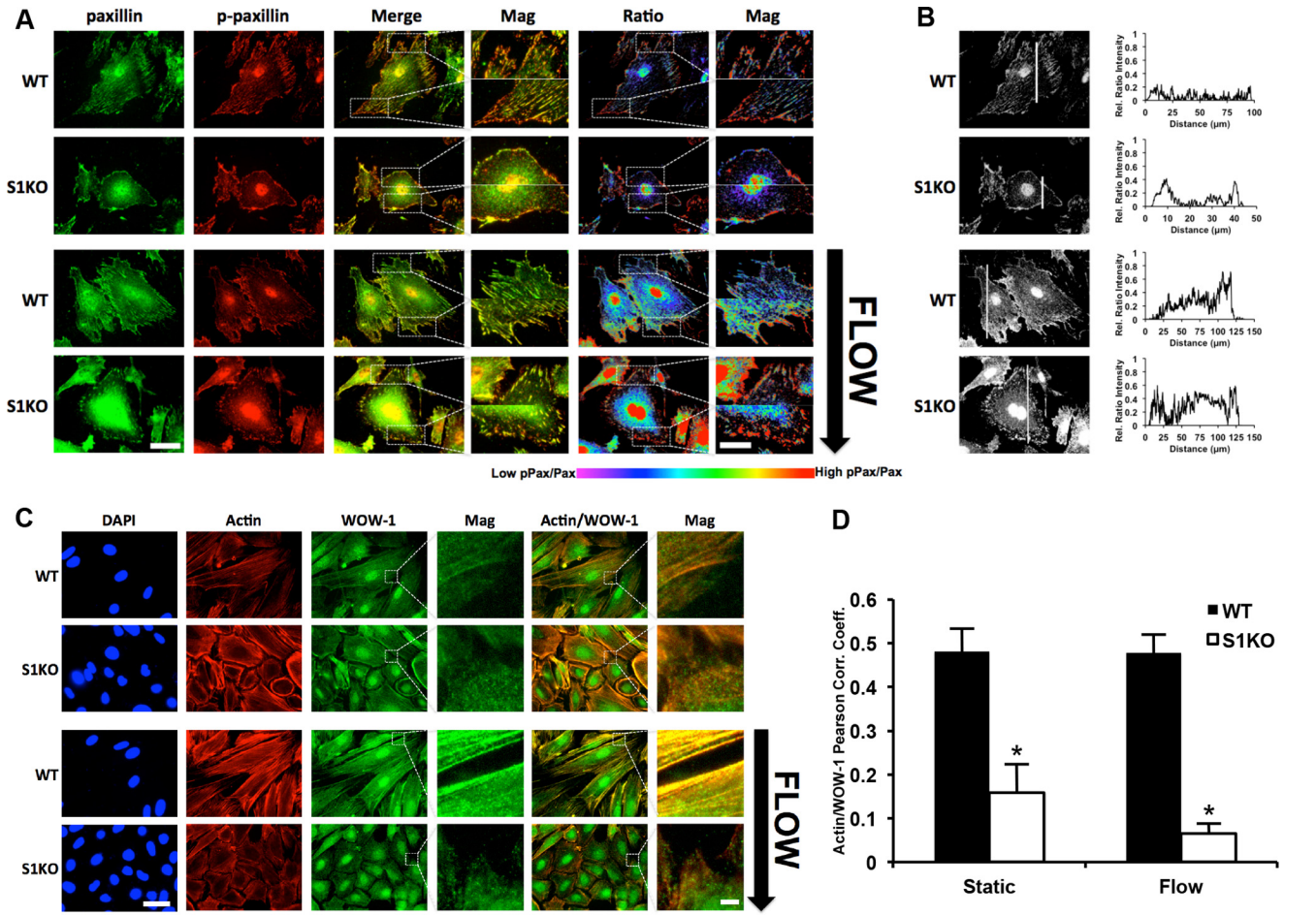

FIGURE 4. **Loss of sdc-1 alters shear stress-induced formation of intracellular spatial gradients in paxillin phosphorylation and reduces active integrin $\alpha_v\beta_3$ association with actin.** *A*, WT and S1KO endothelial cells were exposed to flow at 12 dynes/cm^2 for 15 min. Immunostaining for phosphopaxillin and total paxillin under static and flow conditions shows that WT cells developed a gradient in paxillin phosphorylation across the cell, whereas S1KO cells did not. *Scale bar*, 50 μm in main panel and 25 μm in magnified panel. *B*, line scans of p-paxillin/total paxillin ratio under static and flow illustrate the gradient in paxillin phosphorylation. *C*, actin stress fiber formation and elongation of the cells resulted from 5 min of flow exposure in WT cells. In these cells, activated $\alpha_v\beta_3$ (WOW-1 staining) was colocalized with actin stress fibers, particularly at the periphery of the cell. Knock-out of sdc-1 reduced this association under both static and flow conditions. *Scale bar*, 50 μm in main panel and 5 μm in magnified panel. *D*, colocalization analysis for WOW-1 and actin staining following exposure to flow ($n = 10$). *, statistically significant difference *versus* WT static and flow conditions ($p < 0.05$). *Corr. Coeff.*, correlation coefficient.

(38–40). To measure RhoA activity, we transduced WT and sdc-1 knock-out cells with a retrovirus expressing a RhoA Biosensor (26). The biosensor consists of a single peptide chain containing a Rho-binding domain, cyan fluorescent protein, a randomized linker, yellow fluorescent protein, and RhoA. When RhoA binds GTP and is activated, it binds the Rho-binding domain increasing the FRET efficiency between cyan and yellow fluorescent proteins. We exposed endothelial cells to flow and rapidly measured the RhoA activity using a fluorescence plate reader. A time course of RhoA activity in WT endothelial cells revealed an initial drop in activity followed by an increase to maximum activation after 15 min of flow (Fig. 5). In sdc-1 knock-out endothelial cells exposed to identical flow conditions, there was an initial drop in RhoA activity followed by a return to baseline levels of activity.

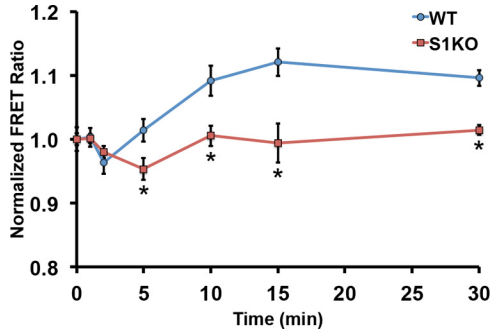

FIGURE 5. **Loss of sdc-1 alters shear stress-induced activation of RhoA.** Endothelial cells were transduced with a RhoA FRET biosensor construct and exposed to flow at 12 dynes/cm^2. The WT cells exhibited a rapid drop in RhoA activity followed by an increase in activity. In contrast, S1KO cells had a rapid drop in activity without a following increase in activity ($n = 6$). *, statistically significant difference *versus* WT group at the same time point ($p < 0.05$).

Long Term Exposure to Flow Produces a Pro-atherosclerotic Phenotype in Syndecan-1 Knock-out Cells—The powerful atheroprotective effects of moderate levels of shear stress result from a broad regulation of genetic programs in endothelial cells that induces an athero-resistant phenotype. Members of the KLF family of transcription factors are key regulators of shear stress-induced changes in endothelial phenotype and are involved in modulation of vasomotor tone, inflammation, and thrombosis (8–11). KLF-2 and KLF-4 have been found to up-regulate genes that are atheroprotective (8–10). In contrast, KLF-5 activates pro-inflammatory gene expression in endothelial cells and

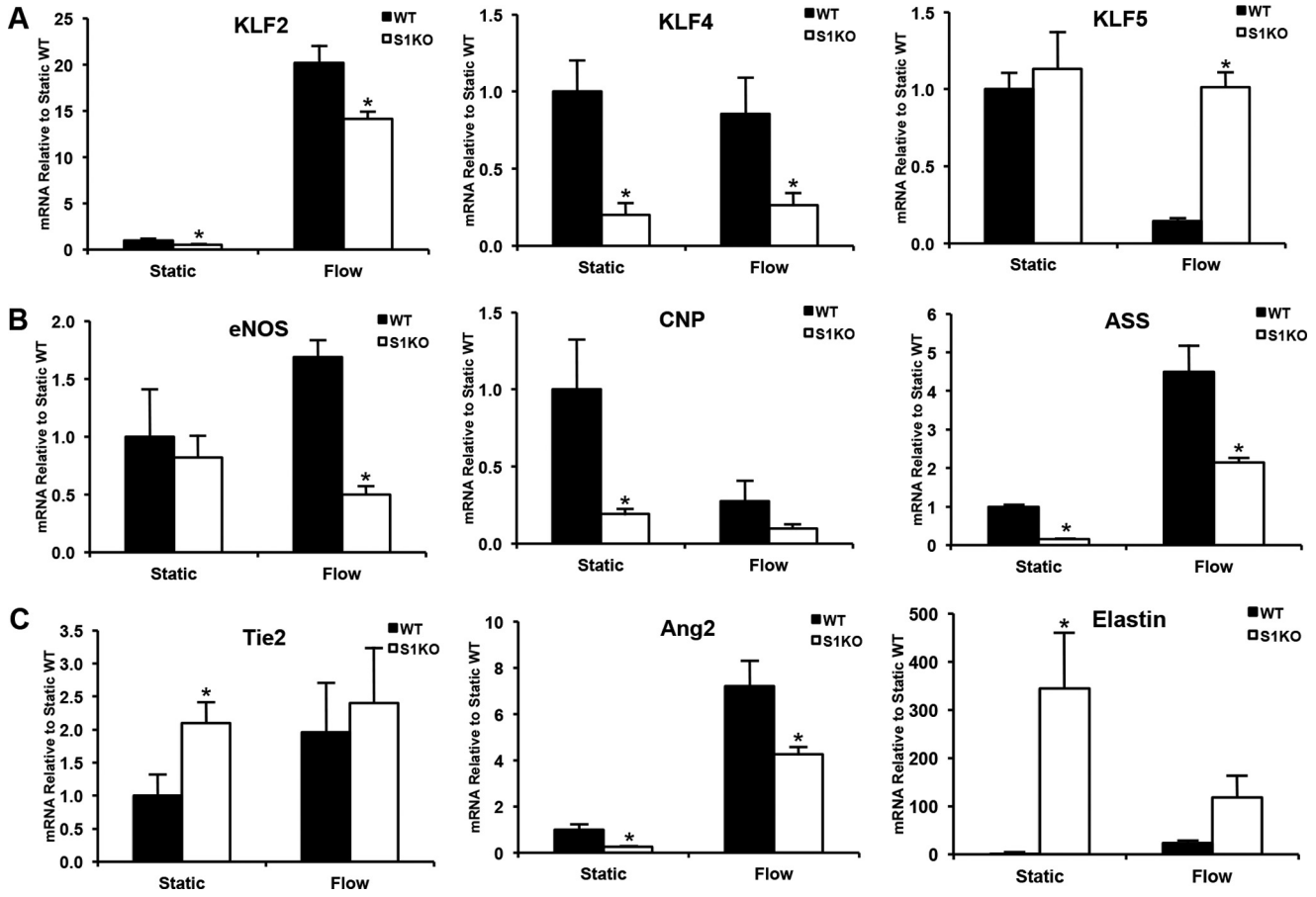

FIGURE 6. **Syndecan-1 alters gene expression for transcription factors, vasodilatory mediators, and angiogenesis factors induced by shear stress.** WT and S1KO endothelial cells were exposed to static conditions or flow at 12 dynes/cm^2 for 24 h. *A*, gene expression for the flow-inducible transcription factors KLF-2 and KLF-4 was decreased for sdc-1 knock-out endothelial cells, whereas KLF-5 expression was increased. *B*, expression of vasodilatory factors was reduced in sdc-1 knock-out cells under atheroprotective flow conditions. *C*, expression of angiogenesis mediators was increased in sdc-1 knock-out cells. *, $p < 0.05$ for S1KO *versus* WT group under same static/flow conditions. *eNOS*, endothelial nitric-oxide synthase; *CNP*, c-natriuretic peptide; *ASS*, argininosuccinate synthetase; *Tie2*, angiopoietin-1 receptor; *Ang2*, angiopoietin-2.

injured arteries (11, 41). We applied 12 dynes/cm^2 of shear stress to endothelial cells for 24 h and measured the gene expression of the KLF transcription factors, vasoregulatory factors, angiogenic factors, and inflammatory mediators. sdc-1 knock-out endothelial cells expressed reduced amounts of KLF-2 and KLF-4 in comparison with WT cells under static and flow conditions (Fig. 6*A*). In addition, treatment with flow reduced expression of KLF-5 in WT cells but not in sdc-1 knock-out cells (Fig. 6*A*). There was decreased expression of vasodilatory factors under atheroprotective flow in sdc-1 knock-out endothelial cells including the genes for endothelial nitric oxide synthase, c-natrietic peptide, and argininosuccinate synthase (Fig. 6*B*). Angiogenesis-related gene expression was increased in sdc-1 knock-out endothelial cells for Tie-2 under static conditions and angiopoietin-2 under both flow and static conditions (Fig. 6*C*). In addition, gene expression for elastin was increased by over 100-fold in sdc-1 cells under static and flow conditions.

Syndecan-1 Knock-out Alters Inflammatory Cytokine Expression—We exposed the endothelial cells to 24 h of laminar flow at 12 dynes/cm^2 and measured the expression of inflammatory cytokines using real time PCR and ELISA. For a subset of these factors including CXCL2, IL-1α, IL-6, and COX-2, we observed lower levels of cytokine expression under static conditions but equal amounts of expression between WT and sdc-1 knock-out cells after exposure to flow (Fig. 7*A*). We found increased expression of CCL-5, IL-15, IP-10, and SDF-1 for sdc-1 knock-out cells under either static or flow conditions or both (Fig. 7*B*). Following exposure to atheroprotective flow, we found increased gene expression for CXCL1, MCP-1, and MIP1-γ (Fig. 8*A*). We performed ELISA for these cytokines on the conditioned media after flow and found they were increased in sdc-1 knock-out cell condition media (Fig. 8*B*).

Syndecan-1 Knock-out Increases Expression of Cell Adhesion Receptors Involved in Leukocyte Adhesion and Increases Adhesion of Cultured Monocytes under Flow—Having observed increased expression of inflammatory factors in sdc-1 knock-out cells, we next examined whether there was regulation of cell adhesion receptors for leukocyte recruitment and a functional difference in the adhesion of monocytes to activated endothelial cells. Under static and atheroprotective flow conditions, we found a 200–300-fold increase in ICAM-1 expression in sdc-1 knock-out cells in comparison with WT cells (Fig. 9*A*). Under atheroprotective flow, sdc-1 knock-out cells had over 4-fold more VCAM-1 gene expression. In addition, we created a lentiviral vector containing the sdc-1 gene and transduced the

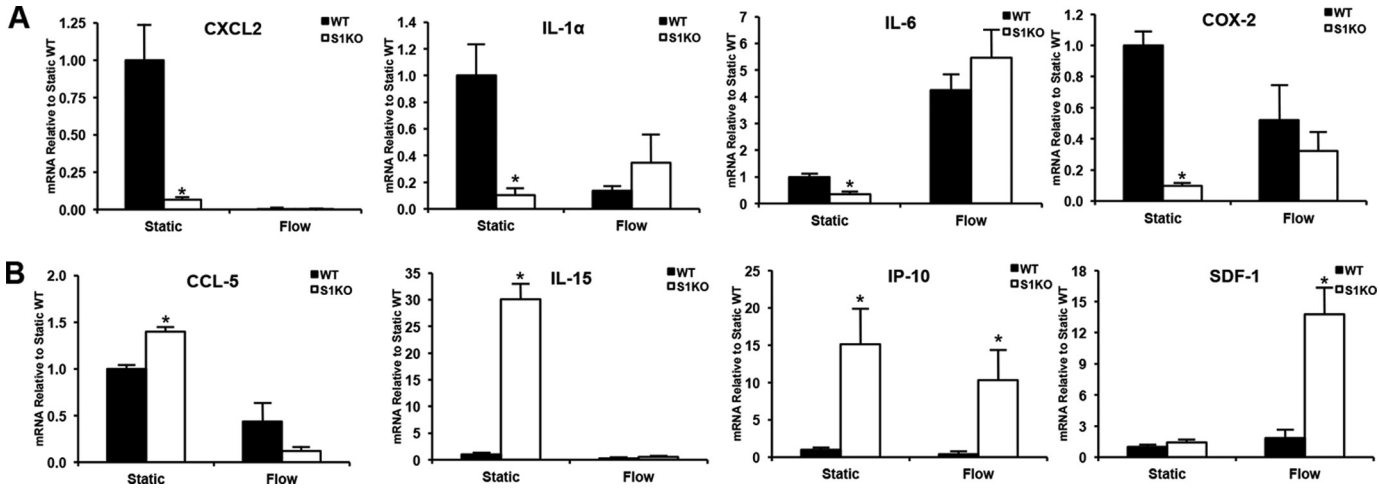

FIGURE 7. **Syndecan-1 knock-out alters baseline and flow-induced cytokine expression.** WT and S1KO endothelial cells were exposed to steady flow at 12 dynes/cm^2 for 24 h. Subsequently, mRNA was isolated and analyzed by real time PCR. *A*, under static conditions S1KO cells had low expression of some inflammatory cytokines including CXCL2, IL-1α, IL-6, and COX-2. These differences were abolished with exposure to flow. *B*, other inflammatory factors were increased under static and/or flow conditions for S1KO cells. *, $p < 0.05$ for S1KO *versus* WT group under same static/flow conditions. *CXCL*, chemokine (C*X*C motif) ligand; *COX-2*, cyclooxygenase-2; *CCL-5*, chemokine (CC motif) ligand 5; *IP-10*, interferon γ-induced protein-10; *SDF-1*, stromal cell-derived factor-1.

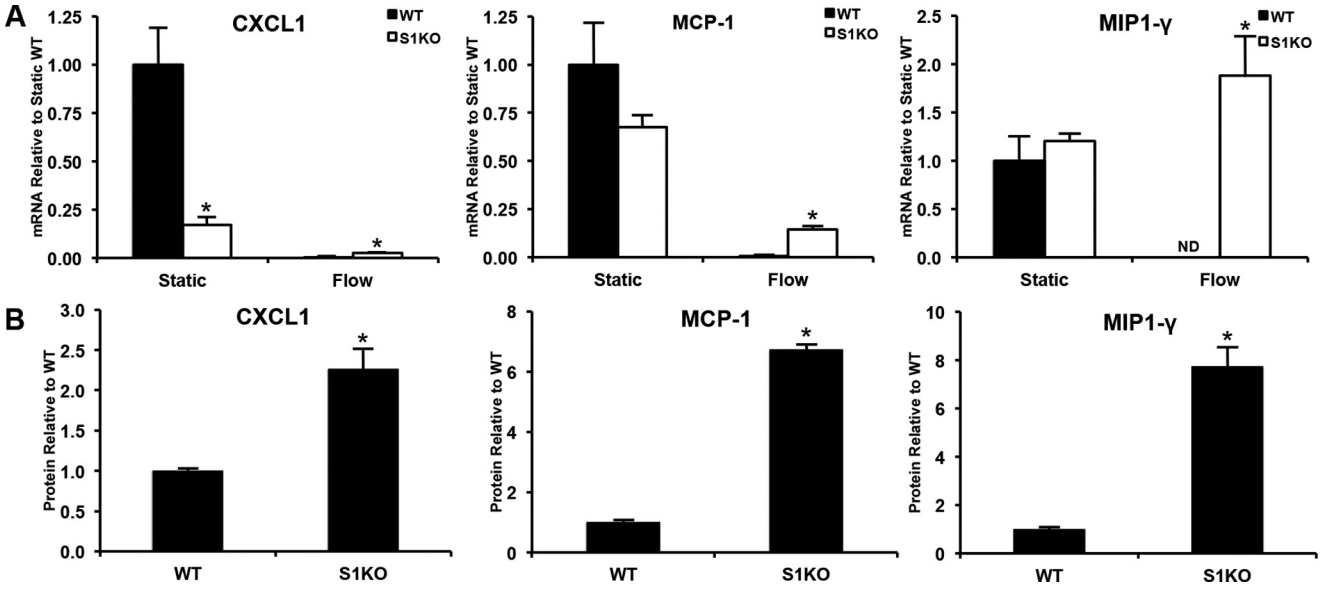

FIGURE 8. **Syndecan-1 knock-out increases gene expression and protein levels of leukocyte recruiting inflammatory soluble factors.** WT and S1KO endothelial cells were exposed to steady flow at 12 dynes/cm^2 for 24 h. Subsequently, mRNA was isolated and analyzed by real time PCR. *A*, gene expression for leukocyte recruiting inflammatory mediators was increased in sdc-1 knock-out cells under flow. *, $p < 0.05$ for S1KO *versus* WT group under same static/flow conditions. *B*, levels of the inflammatory factors were assessed in the culture media following 24 h of flow using ELISA. *, statistically significant difference ($p < 0.05$) for S1KO *versus* WT cells. *CXCL1*, chemokine (C*X*C motif) ligand-1; *MCP-1*, monocyte chemotactic protein-1; *MIP1-γ*, macrophage inflammatory protein 1γ.

sdc-1 knock-out line with this construct (pSyn1). Although ICAM-1 levels remained elevated, VCAM-1 and E-selectin expression levels were reduced in the pSyn1 model.

We next examined the functional consequences of sdc-1 knock-out on monocyte adhesion *in vitro*. We fluorescently labeled cultured monocytes and measured their adhesion to a TNF-α stimulated endothelial monolayer under flow conditions (0.5 dynes/cm^2 for 5 min). Approximately 50-fold more monocytes adhered to sdc-1 knock-out endothelial monolayers than to WT monolayers under identical flow conditions (Fig. 9, *B* and *C*). More cells were also observed to roll on sdc-1 knock-out monolayers during the flow adhesion assay (Fig. 9*D* and supplemental Videos 1–3). Overexpression of sdc-1 in the knock-out cells using lentiviral transduction reduced the number of adhered monocytes by approximately half in comparison with sdc-1 knock-out cells (Fig. 9, *C* and *D*).

Syndecan-1 Knock-out Mice Have Increased Leukocyte Recruitment and Inflammatory Response—To examine whether the changes in inflammatory state in our cultured endothelial cells were recapitulated *in vivo*, we injected WT and sdc-1 knock-out mice intraperitoneally with thioglycolate medium to induce the recruitment of macrophages. After 4 days, we collected the recruited cells by intraperitoneal lavage and found a 2-fold increase in macrophage recruitment in sdc-1 knock-out mice using FACS analysis for CD14-stained cells (Fig. 10*A*). We next examined the functional response of sdc-1 knock-out mice to a

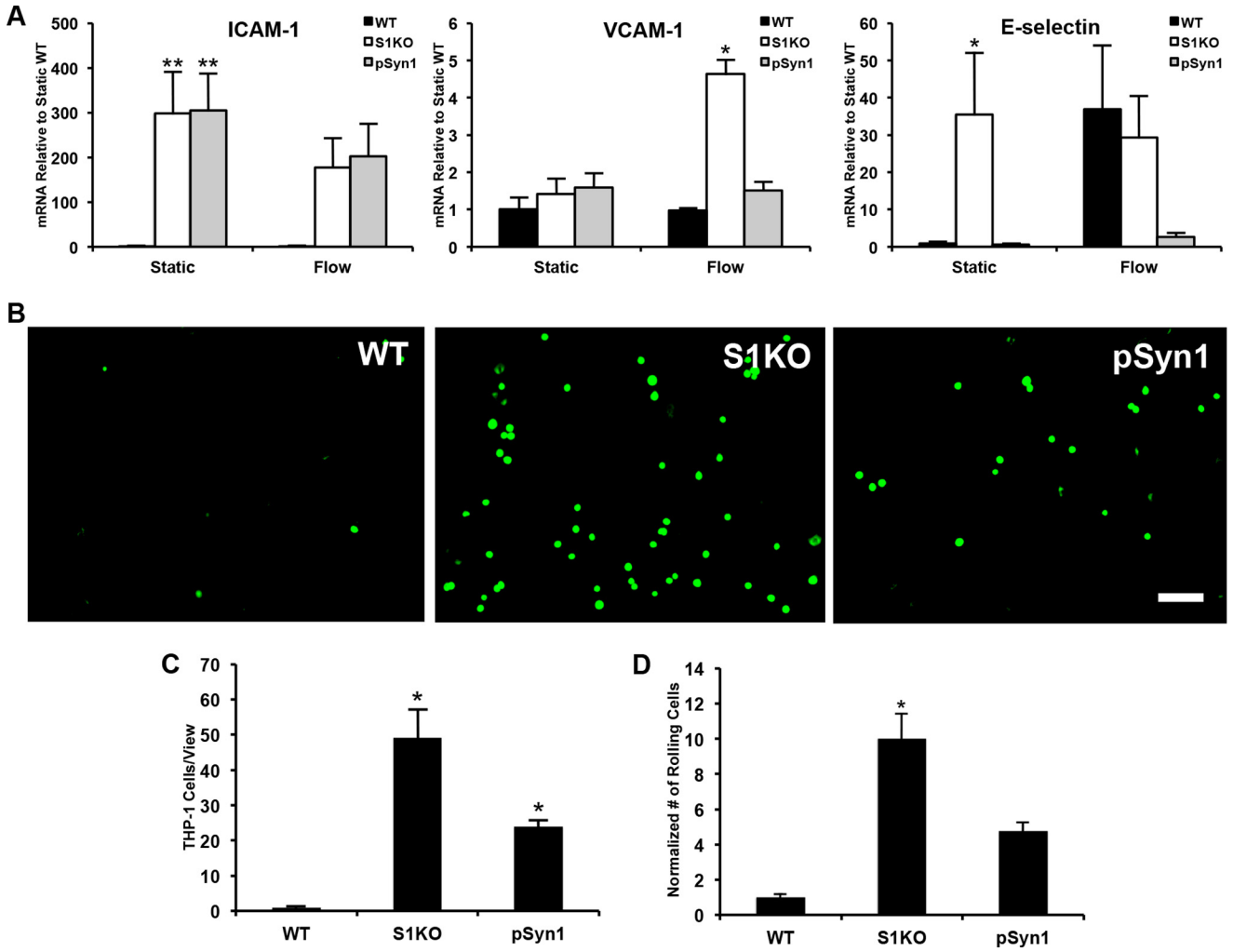

FIGURE 9. **Monocyte adhesion and macrophage recruitment are increased in sdc-1 knock-out endothelial cells.** *A*, WT and S1KO endothelial cells were exposed to 24 h of flow at 12 dynes/cm^2. Gene expression for cell adhesion receptors was higher in the S1KO cells compared with WT cells following flow exposure. *, $p < 0.05$ in comparison with all other groups in static or flow; **, $p < 0.05$ in comparison with WT in static or flow. *B*, suspension cultured monocytes were fluorescently labeled and flowed over confluent endothelial monolayers of WT, S1KO, or S1KO cells transduced to overexpress sdc-1 (pSyn1) under flow creating 0.5 dynes/cm^2 of shear stress for 5 min. Prior to the flow adhesion assay, the endothelial cells were stimulated with TNF-α for 4 h. *Scale bar*, 200 μm. *C*, leukocyte adhesion was increased in sdc-1 knock-out cells, and re-expression of sdc-1 in these cells decreased the number adhering leukocytes ($n = 8$). *, $p < 0.05$ in comparison with all other groups. *D*, the number of rolling monocytes over three 90-s intervals shows increased leukocyte rolling on sdc-1 knock-out cells over both WT and pSyn1 cell line. *, statistically different from all other groups ($p < 0.05$).

vasodilatory/inflammatory stimulus. We applied mustard oil to the feet of anesthetized mice and measured the increase in blood flow over time using laser speckle imaging. We found that sdc-1 knock-out mice had a greater increase in perfusion in response to the same level of treatment with mustard oil (Fig. 10, *B* and *C*). Histological analysis revealed qualitatively greater edema in the feet of sdc-1 knock-out mice in comparison with WT mice (Fig. 10*D*).

DISCUSSION

Although the role of cell surface proteoglycans in shear stress sensing has been suspected for many years (1) there have been no studies, to our knowledge, that have examined their function in a mechanistic and detailed fashion. The primary experimental approach in studies to date has been to digest particular glycosaminoglycans of the glycocalyx using enzymes and to apply shear stress to interrogate whether the shear sensing of endothelial cells has changed from this treatment. Using this method, several studies have shown that shear stress-induced production of NO is reduced following enzymatic digestion of heparan sulfate or hyaluronic acid or treatment with neuraminidase (15, 42). In contrast, shear-induced increases in prostacyclin-2 were not affected by removal of heparan sulfate, sialic acid, chondroitin sulfate, or hyaluronan (43). *In vivo* studies have also supported the involvement of proteoglycans in controlling shear stress-induced arterial vasodilation. Increases in blood flow cause arteries to dilate in an endothelium-dependent manner (44, 45). Several studies have supported the role of elements of the glycocalyx in the control of the shear-induced vasodilatory response of arteries. Another study examined the vasoconstriction of rabbit femoral arteries in *ex vivo* organ culture and found that incubation with neuraminidase, an enzyme that digests sialic acid moieties, reduced shear stress-induced NO release (46). In addition, treatment with clinical levels of heparin led to a reduction in the duration of vasodilation in response to occlusion-induced reactive hyperemia in mice (47).

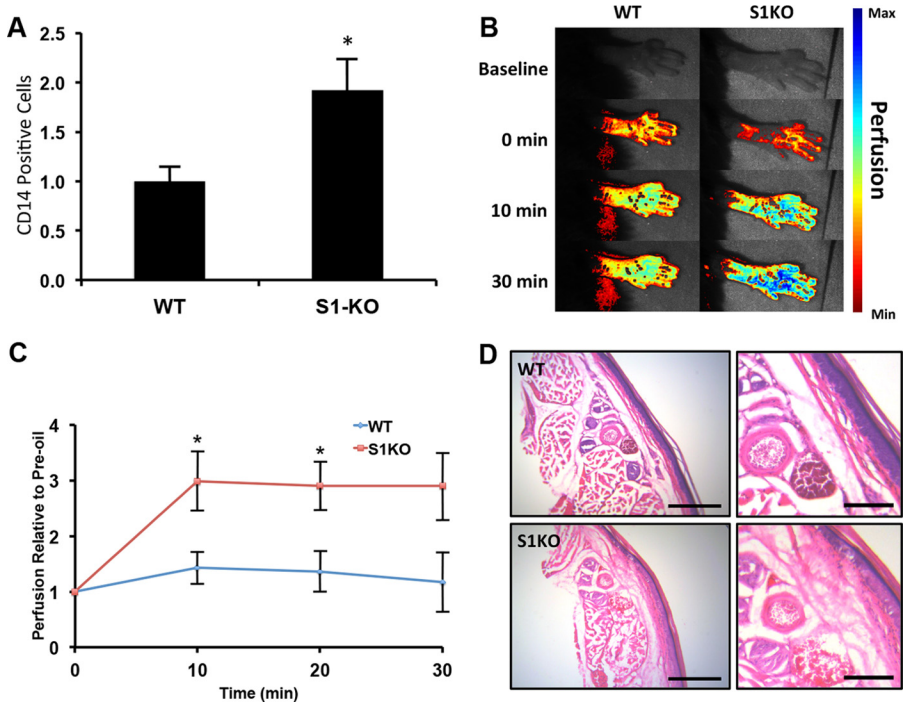

FIGURE 10. **Inflammatory responsiveness is increased in sdc-1 knock-out mice.** *A*, WT and S1KO mice were given an injection of thioglycolate, and the number of recruited macrophages was measured using FACS after 4 days. sdc-1 mice had an increased number of macrophages recruited to the injection site. *, $p < 0.05$ *versus* WT group. *B*, the foot pads of mice were treated with mustard oil (allyl isothiocyanate), and the response was measured by tracking tissue perfusion using laser speckle flow imaging. sdc-1 knock-out mice had an increased response to the mustard oil. *C*, the S1KO mice showed an increase in relative blood perfusion relative to the WT mice. *, $p < 0.05$ *versus* WT group at given time point. *D*, histological analysis of the foot pads of WT and S1KO mice after H&E staining. *Scale bar*, 400 μm in main panel and 150 μm in magnified panel.

Our study adds to these results by defining several of the activities of sdc-1 in the initial steps of mechanosensing and in the regulation of endothelial phenotype.

We first examined the role of sdc-1 in the acute mechanosensing of shear stresses by endothelial cells. Interestingly, without sdc-1, endothelial cells were not able to activate Akt and RhoA nor develop a paxillin phosphorylation gradient in response to flow. These signaling events have been shown in previous studies to be key to flow-induced changes in endothelial alignment (34) and cytoskeletal remodeling (38–40), as well as the regulation of oxidative stress (31), cell survival (32), and production of NO (33). Our study also examined the longer term effects of shear stress on endothelial cells in the absence of sdc-1 expression. Under atheroprotective flow, sdc-1 knock-out cells had decreased expression of atheroprotective transcription factors KLF-2 and KLF-4. These transcription factors regulate a set of genetic programs that profoundly alter the endothelial cell phenotype affecting pathways involved in inflammation, vasodilation, and thrombosis (8–10). In contrast we found that KLF-5 expression was higher in sdc-1 knock-out endothelial cells after exposure to flow. This transcription factor has been linked to increased inflammation in endothelial cells (11, 41). Thus, the loss of sdc-1 alters the relative expression of KLF transcription factors and their regulation by atheroprotective flow. Consistent with these findings, sdc-1 knock-out cells had increased expression of pro-inflammatory genes, cytokines, and leukocyte adhesion receptors in comparison with WT cells. The functional result of these alterations in endothelial genetic programs was an increased leukocyte adhesion and an increased responsiveness to inflammatory stimuli *in vivo*.

Taken together, our results suggest an atheroprotective role for sdc-1 with its expression supporting flow-mediated mechanosensing and the generation of the atheroprotective phenotype. Loss of sdc-1 also induced significant differences in baseline levels of many markers of endothelial phenotype. In the absence of flow, we found decreased levels of gene expression for KLF-4, c-natriuretic peptide, argininosuccinate synthase-1, angiopoietin-2, and several of the inflammatory cytokines including CXCL1 and CXCL2. In contrast, under static conditions there was significantly increased gene expression for elastin, CCL-5, IL-15, IP-10, and ICAM-1. Thus, the effect of sdc-1 loss on flow-mediated signaling and phenotypic regulation should not be viewed as a simple effect of altered endothelial mechanotransduction but in the context of significant dysregulation of endothelial cell phenotype under baseline conditions. It should also be noted that the loss of sdc-1 leads to an increase in gene expression of the other glycocalyx components, specifically sdc-4 and gpc-1, as well as numerous sulfotransferases involved in heparan sulfate synthesis. We believe this to be a compensatory mechanism; however, the mechanotransduction effects we observed despite this response further highlight the importance of sdc-1 in signal transduction.

Several recent studies have found results that are consistent and complementary to our findings here. Notably, a recent study identified that, among several proteoglycan core proteins, sdc-1 expression was specifically reduced in endothelial cells on exposure to atheroprone regimes of flow and increased under

atheroprotective flow conditions (48). Viewed from the context of our results, these findings would suggest that regulation of sdc-1 by flow could contribute to the atherosclerosis and the development of endothelial dysfunction. In addition, another study found that the glycocalyx in sdc-1 knock-out mice was thinner than in WT mice using intravital microscopy (49). They also observed an increased number of leukocytes adhered in the venules of the mice, consistent with our findings of increased leukocyte adhesion *in vitro* and recruitment in *in vivo* studies. In the context of these results, our studies support that loss of sdc-1 stimulated by exposure to atherogenic flow profiles would lead endothelial cells to adopt an atheroprone phenotype that is both pro-inflammatory and resistant to the anti-inflammatory stimulus of moderate shear stress.

Our findings also have several important implications for the understanding of vascular biology in the context of atherogenesis and inflammation. sdc-1 and the other syndecan family members are highly sensitive to proteolytic degradation and shedding (50). Thus, our findings imply that disease-induced increases in proteolytic activity leading to shedding of sdc-1 from the surface may alter endothelial inflammatory phenotype and shear sensitivity to atheroprotective flow. We have recently found that Ob/Ob mice given a high fat diet have lower levels of sdc-1 protein in their heart and skeletal muscle (51). In addition, sdc-1 is a target for heparanase activity and leads to shedding from the cell surface (52). Our group has recently identified a key role for the enzyme heparanase in restenosis and thrombosis in vascular injury (53, 54). We also found increased heparanase expression in severe atherosclerotic plaques and in arterial segments of the coronary vessels with low shear stress in a diabetic, hyperlipidemic porcine model of atherosclerosis (27). This finding has recently been corroborated in atherosclerotic plaques from human patients (55). Another study has also identified heparanase to be key in controlling the inflammatory response in sepsis through degradation of the glycocalyx (56). Thus, our findings suggest that heparanase/protease-induced shedding of sdc-1 could lead to modulation of endothelial phenotype and inflammatory properties potentially similar to our sdc-1 knock-out cells in this study.

It should be noted that one potential limitation of our studies is the use of cultured cells to study the function of glycocalyx components. Cultured cells are known to have limited formation of glycocalyx in comparison with the extended structure found in *in vivo* vessels (57, 58). Thus, although our findings support a functional role sdc-1, they do not rigorously substantiate it in the presence of the full glycocalyx structure that is present in *in vivo* conditions. Additionally, whereas the lentiviral overexpression of sdc-1 is highly effective in expressing the protein in knock-out cells, it also has some limitations. Namely, having high levels of sdc-1 may disrupt the normal function of the protein and overwhelm the heparan sulfate synthetic enzymes that perform the post-translational modification of the protein. In addition, sdc-1 is a ligand for the viral entry of the HIV lentivirus. Thus, there may be effects on this system from the cell response to lentiviral transduction. These mechanisms may, in part, explain why there is a partial, but not complete, reduction of leukocyte adhesion by sdc-1 overexpression.

In summary, our study demonstrates that sdc-1 is a key element in endothelial mechanosensing and suggests an atheroprotective role for sdc-1 in flow-mediated endothelial phenotypic regulation. Our work supports that loss of sdc-1 from the endothelial surface leads to the adoption of a pro-inflammatory phenotype that is dysregulated in response to the atheroprotective effects of flow. Many disease states increase the expression of enzymes that could induce the shedding and degradation of sdc-1 causing its loss from the endothelial surface (51, 59, 60). Thus, therapies that preserve or enhance sdc-1 on the endothelial surface, either through increased expression or inhibition of shedding, may have potential in preventing the early stages of atherogenesis and enhancing the atheroprotective effects of shear stress.

REFERENCES

1. Davies, P. F., Barbee, K. A., Volin, M. V., Robotewskyj, A., Chen, J., Joseph, L., Griem, M. L., Wernick, M. N., Jacobs, E., Polacek, D. C., dePaola, N., and Barakat, A. I. (1997) Spatial relationships in early signaling events of flow-mediated endothelial mechanotransduction. *Annu. Rev. Physiol.* **59,** 527–549
2. Hahn, C., and Schwartz, M. A. (2009) Mechanotransduction in vascular physiology and atherogenesis. *Nat. Rev. Mol. Cell Biol.* **10,** 53–62
3. Hoger, J. H., Ilyin, V. I., Forsyth, S., and Hoger, A. (2002) Shear stress regulates the endothelial Kir2.1 ion channel. *Proc. Natl. Acad. Sci. U.S.A.* **99,** 7780–7785
4. Hutcheson, I. R., and Griffith, T. M. (1996) Mechanotransduction through the endothelial cytoskeleton: mediation of flow- but not agonist-induced EDRF release. *Br. J. Pharmacol.* **118,** 720–726
5. Iomini, C., Tejada, K., Mo, W., Vaananen, H., and Piperno, G. (2004) Primary cilia of human endothelial cells disassemble under laminar shear stress. *J. Cell Biol.* **164,** 811–817
6. Malek, A. M., Zhang, J., Jiang, J., Alper, S. L., and Izumo, S. (1999) Endothelin-1 gene suppression by shear stress: pharmacological evaluation of the role of tyrosine kinase, intracellular calcium, cytoskeleton, and mechanosensitive channels. *J. Mol. Cell. Cardiol.* **31,** 387–399
7. Schwartz, M. A., and DeSimone, D. W. (2008) Cell adhesion receptors in mechanotransduction. *Curr. Opin. Cell Biol.* **20,** 551–556
8. Parmar, K. M., Larman, H. B., Dai, G., Zhang, Y., Wang, E. T., Moorthy, S. N., Kratz, J. R., Lin, Z., Jain, M. K., Gimbrone, M. A., Jr., and García-Cardeña, G. (2006) Integration of flow-dependent endothelial phenotypes by Kruppel-like factor 2. *J. Clin. Invest.* **116,** 49–58
9. Hamik, A., Lin, Z., Kumar, A., Balcells, M., Sinha, S., Katz, J., Feinberg, M. W., Gerzsten, R. E., Edelman, E. R., and Jain, M. K. (2007) Kruppel-like factor 4 regulates endothelial inflammation. *J. Biol. Chem.* **282,** 13769–13779
10. Zhou, G., Hamik, A., Nayak, L., Tian, H., Shi, H., Lu, Y., Sharma, N., Liao, X., Hale, A., Boerboom, L., Feaver, R. E., Gao, H., Desai, A., Schmaier, A., Gerson, S. L., Wang, Y., Atkins, G. B., Blackman, B. R., Simon, D. I., and Jain, M. K. (2012) Endothelial Kruppel-like factor 4 protects against atherothrombosis in mice. *J. Clin. Invest.* **122,** 4727–4731
11. Kumekawa, M., Fukuda, G., Shimizu, S., Konno, K., and Odawara, M. (2008) Inhibition of monocyte chemoattractant protein-1 by Kruppel-like factor 5 small interfering RNA in the tumor necrosis factor-α-activated human umbilical vein endothelial cells. *Biol. Pharm. Bull.* **31,** 1609–1613
12. Tzima, E., Irani-Tehrani, M., Kiosses, W. B., Dejana, E., Schultz, D. A., Engelhardt, B., Cao, G., DeLisser, H., and Schwartz, M. A. (2005) A mechanosensory complex that mediates the endothelial cell response to fluid shear stress. *Nature* **437,** 426–431
13. Ebong, E. E., Macaluso, F. P., Spray, D. C., and Tarbell, J. M. (2011) Imaging the endothelial glycocalyx in vitro by rapid freezing/freeze substitution transmission electron microscopy. *Arterioscler. Thromb. Vasc. Biol.* **31,** 1908–1915
14. Weinbaum, S., Zhang, X., Han, Y., Vink, H., and Cowin, S. C. (2003) Mechanotransduction and flow across the endothelial glycocalyx. *Proc.*

Natl. Acad. Sci. U.S.A. **100,** 7988–7995
15. Florian, J. A., Kosky, J. R., Ainslie, K., Pang, Z., Dull, R. O., and Tarbell, J. M. (2003) Heparan sulfate proteoglycan is a mechanosensor on endothelial cells. *Circ. Res.* **93,** e136–142
16. Bishop, J. R., Schuksz, M., and Esko, J. D. (2007) Heparan sulphate proteoglycans fine-tune mammalian physiology. *Nature* **446,** 1030–1037
17. Hsia, E., Richardson, T. P., and Nugent, M. A. (2003) Nuclear localization of basic fibroblast growth factor is mediated by heparan sulfate proteoglycans through protein kinase C signaling. *J. Cell. Biochem.* **88,** 1214–1225
18. Tkachenko, E., Rhodes, J. M., and Simons, M. (2005) Syndecans: new kids on the signaling block. *Circ. Res.* **96,** 488–500
19. Rapraeger, A. C. (2013) Synstatin: a selective inhibitor of the syndecan-1-coupled IGF1R-$\alpha v\beta 3$ integrin complex in tumorigenesis and angiogenesis. *FEBS J.* **280,** 2207–2215
20. Okina, E., Manon-Jensen, T., Whiteford, J. R., and Couchman, J. R. (2009) Syndecan proteoglycan contributions to cytoskeletal organization and contractility. *Scand. J. Med. Sci. Sports* **19,** 479–489
21. Roper, J. A., Williamson, R. C., and Bass, M. D. (2012) Syndecan and integrin interactomes: large complexes in small spaces. *Curr. Opin. Struct. Biol.* **22,** 583–590
22. Dong, Q. G., Bernasconi, S., Lostaglio, S., De Calmanovici, R. W., Martin-Padura, I., Breviario, F., Garlanda, C., Ramponi, S., Mantovani, A., and Vecchi, A. (1997) A general strategy for isolation of endothelial cells from murine tissues. Characterization of two endothelial cell lines from the murine lung and subcutaneous sponge implants. *Arterioscler. Thromb. Vasc. Biol.* **17,** 1599–1604
23. Mostoslavsky, G., Kotton, D. N., Fabian, A. J., Gray, J. T., Lee, J. S., and Mulligan, R. C. (2005) Efficiency of transduction of highly purified murine hematopoietic stem cells by lentiviral and oncoretroviral vectors under conditions of minimal in vitro manipulation. *Mol. Ther.* **11,** 932–940
24. Voyvodic, P. L., Min, D., and Baker, A. B. (2012) A multichannel dampened flow system for studies on shear stress-mediated mechanotransduction. *Lab Chip* **12,** 3322–3330
25. Baker, A. B., Ettenson, D. S., Jonas, M., Nugent, M. A., Iozzo, R. V., and Edelman, E. R. (2008) Endothelial cells provide feedback control for vascular remodeling through a mechanosensitive autocrine TGF-β signaling pathway. *Circ. Res.* **103,** 289–297
26. Pertz, O., Hodgson, L., Klemke, R. L., and Hahn, K. M. (2006) Spatiotemporal dynamics of RhoA activity in migrating cells. *Nature* **440,** 1069–1072
27. Koskinas, K. C., Feldman, C. L., Chatzizisis, Y. S., Coskun, A. U., Jonas, M., Maynard, C., Baker, A. B., Papafaklis, M. I., Edelman, E. R., and Stone, P. H. (2010) Natural history of experimental coronary atherosclerosis and vascular remodeling in relation to endothelial shear stress: a serial, *in vivo* intravascular ultrasound study. *Circulation* **121,** 2092–2101
28. Chatzizisis, Y. S., Baker, A. B., Sukhova, G. K., Koskinas, K. C., Papafaklis, M. I., Beigel, R., Jonas, M., Coskun, A. U., Stone, B. V., Maynard, C., Shi, G. P., Libby, P., Feldman, C. L., Edelman, E. R., and Stone, P. H. (2011) Augmented expression and activity of extracellular matrix-degrading enzymes in regions of low endothelial shear stress colocalize with coronary atheromata with thin fibrous caps in pigs. *Circulation* **123,** 621–630
29. Alexander, C. M., Reichsman, F., Hinkes, M. T., Lincecum, J., Becker, K. A., Cumberledge, S., and Bernfield, M. (2000) Syndecan-1 is required for Wnt-1-induced mammary tumorigenesis in mice. *Nat. Genet.* **25,** 329–332
30. Dunn, A. K. (2012) Laser speckle contrast imaging of cerebral blood flow. *Ann. Biomed. Eng.* **40,** 367–377
31. Dai, G., Vaughn, S., Zhang, Y., Wang, E. T., Garcia-Cardena, G., and Gimbrone, M. A., Jr. (2007) Biomechanical forces in atherosclerosis-resistant vascular regions regulate endothelial redox balance via phosphoinositol 3-kinase/Akt-dependent activation of Nrf2. *Circ. Res.* **101,** 723–733
32. Dimmeler, S., Assmus, B., Hermann, C., Haendeler, J., and Zeiher, A. M. (1998) Fluid shear stress stimulates phosphorylation of Akt in human endothelial cells: involvement in suppression of apoptosis. *Circ. Res.* **83,** 334–341
33. Dimmeler, S., Fleming, I., Fisslthaler, B., Hermann, C., Busse, R., and Zeiher, A. M. (1999) Activation of nitric oxide synthase in endothelial cells by Akt-dependent phosphorylation. *Nature* **399,** 601–605
34. Zaidel-Bar, R., Kam, Z., and Geiger, B. (2005) Polarized downregulation of the paxillin-p130CAS-Rac1 pathway induced by shear flow. *J. Cell Sci.* **118,** 3997–4007
35. Orr, A. W., Ginsberg, M. H., Shattil, S. J., Deckmyn, H., and Schwartz, M. A. (2006) Matrix-specific suppression of integrin activation in shear stress signaling. *Mol. Biol. Cell* **17,** 4686–4697
36. Hennig, T., Mogensen, C., Kirsch, J., Pohl, U., and Gloe, T. (2011) Shear stress induces the release of an endothelial elastase: role in integrin $\alpha_v\beta_3$-mediated FGF-2 release. *J. Vasc. Res.* **48,** 453–464
37. Pampori, N., Hato, T., Stupack, D. G., Aidoudi, S., Cheresh, D. A., Nemerow, G. R., and Shattil, S. J. (1999) Mechanisms and consequences of affinity modulation of integrin $\alpha_v\beta_3$ detected with a novel patch-engineered monovalent ligand. *J. Biol. Chem.* **274,** 21609–21616
38. Cicha, I., Goppelt-Struebe, M., Muehlich, S., Yilmaz, A., Raaz, D., Daniel, W. G., and Garlichs, C. D. (2008) Pharmacological inhibition of RhoA signaling prevents connective tissue growth factor induction in endothelial cells exposed to non-uniform shear stress. *Atherosclerosis* **196,** 136–145
39. Yang, B., Radel, C., Hughes, D., Kelemen, S., and Rizzo, V. (2011) p190 RhoGTPase-activating protein links the β1 integrin/caveolin-1 mechanosignaling complex to RhoA and actin remodeling. *Arterioscler. Thromb. Vasc. Biol.* **31,** 376–383
40. Tzima, E. (2006) Role of small GTPases in endothelial cytoskeletal dynamics and the shear stress response. *Circ. Res.* **98,** 176–185
41. Hoshino, Y., Kurabayashi, M., Kanda, T., Hasegawa, A., Sakamoto, H., Okamoto, E., Kowase, K., Watanabe, N., Manabe, I., Suzuki, T., Nakano, A., Takase, S., Wilcox, J. N., and Nagai, R. (2000) Regulated expression of the BTEB2 transcription factor in vascular smooth muscle cells: analysis of developmental and pathological expression profiles shows implications as a predictive factor for restenosis. *Circulation* **102,** 2528–2534
42. Kumagai, R., Lu, X., and Kassab, G. S. (2009) Role of glycocalyx in flow-induced production of nitric oxide and reactive oxygen species. *Free Radic. Biol. Med.* **47,** 600–607
43. Pahakis, M. Y., Kosky, J. R., Dull, R. O., and Tarbell, J. M. (2007) The role of endothelial glycocalyx components in mechanotransduction of fluid shear stress. *Biochem. Biophys. Res. Commun.* **355,** 228–233
44. Pohl, U., Herlan, K., Huang, A., and Bassenge, E. (1991) EDRF-mediated shear-induced dilation opposes myogenic vasoconstriction in small rabbit arteries. *Am. J. Physiol.* **261,** H2016–H2023
45. Kamiya, A., Bukhari, R., and Togawa, T. (1984) Adaptive regulation of wall shear stress optimizing vascular tree function. *Bull. Math. Biol.* **46,** 127–137
46. Hecker, M., Mülsch, A., Bassenge, E., and Busse, R. (1993) Vasoconstriction and increased flow: two principal mechanisms of shear stress-dependent endothelial autacoid release. *Am. J. Physiol.* **265,** H828–H833
47. Van Teeffelen, J. W., Brands, J., Stroes, E. S., and Vink, H. (2007) Endothelial glycocalyx: sweet shield of blood vessels. *Trends. Cardiovasc. Med.* **17,** 101–105
48. Koo, A., Dewey, C. F., Jr., and García-Cardeña, G. (2013) Hemodynamic shear stress characteristic of atherosclerosis-resistant regions promotes glycocalyx formation in cultured endothelial cells. *Am. J. Physiol. Cell Physiol.* **304,** C137–C146
49. Savery, M. D., Jiang, J. X., Park, P. W., and Damiano, E. R. (2013) The endothelial glycocalyx in syndecan-1 deficient mice. *Microvasc. Res.* **87,** 83–91
50. Nam, E. J., and Park, P. W. (2012) Shedding of cell membrane-bound proteoglycans. *Methods Mol. Biol.* **836,** 291–305
51. Das, S., Singh, G., and Baker, A. B. (2014) Overcoming disease-induced growth factor resistance in therapeutic angiogenesis using recombinant co-receptors delivered by a liposomal system. *Biomaterials* **35,** 196–205
52. Ramani, V. C., Purushothaman, A., Stewart, M. D., Thompson, C. A., Vlodavsky, I., Au, J. L., and Sanderson, R. D. (2013) The heparanase/syndecan-1 axis in cancer: mechanisms and therapies. *FEBS J.* **280,** 2294–2306
53. Baker, A. B., Gibson, W. J., Kolachalama, V. B., Golomb, M., Indolfi, L., Spruell, C., Zcharia, E., Vlodavsky, I., and Edelman, E. R. (2012) Heparanase regulates thrombosis in vascular injury and stent-induced flow disturbance. *J. Am. Coll. Cardiol.* **59,** 1551–1560

54. Mobine, H. R., Baker, A. B., Wang, L., Wakimoto, H., Jacobsen, K. C., Seidman, C. E., Seidman, J. G., and Edelman, E. R. (2009) Pheochromocytoma-induced cardiomyopathy is modulated by the synergistic effects of cell-secreted factors. *Circ. Heart. Fail.* **2,** 121–128
55. Blich, M., Golan, A., Arvatz, G., Sebbag, A., Shafat, I., Sabo, E., Cohen-Kaplan, V., Petcherski, S., Avniel-Polak, S., Eitan, A., Hammerman, H., Aronson, D., Axelman, E., Ilan, N., Nussbaum, G., and Vlodavsky, I. (2013) Macrophage activation by heparanase is mediated by TLR-2 and TLR-4 and associates with plaque progression. *Arterioscler. Thromb. Vasc. Biol.* **33,** e56–e65
56. Schmidt, E. P., Yang, Y., Janssen, W. J., Gandjeva, A., Perez, M. J., Barthel, L., Zemans, R. L., Bowman, J. C., Koyanagi, D. E., Yunt, Z. X., Smith, L. P., Cheng, S. S., Overdier, K. H., Thompson, K. R., Geraci, M. W., Douglas, I. S., Pearse, D. B., and Tuder, R. M. (2012) The pulmonary endothelial glycocalyx regulates neutrophil adhesion and lung injury during experimental sepsis. *Nat. Med.* **18,** 1217–1223
57. Potter, D. R., and Damiano, E. R. (2008) The hydrodynamically relevant endothelial cell glycocalyx observed *in vivo* is absent *in vitro*. *Circ. Res.* **102,** 770–776
58. Potter, D. R., Jiang, J., and Damiano, E. R. (2009) The recovery time course of the endothelial cell glycocalyx *in vivo* and its implications in vitro. *Circ. Res.* **104,** 1318–1325
59. Baker, A. B., Chatzizisis, Y. S., Beigel, R., Jonas, M., Stone, B. V., Coskun, A. U., Maynard, C., Rogers, C., Koskinas, K. C., Feldman, C. L., Stone, P. H., and Edelman, E. R. (2010) Regulation of heparanase expression in coronary artery disease in diabetic, hyperlipidemic swine. *Atherosclerosis* **213,** 436–442
60. Baker, A. B., Groothuis, A., Jonas, M., Ettenson, D. S., Shazly, T., Zcharia, E., Vlodavsky, I., Seifert, P., and Edelman, E. R. (2009) Heparanase alters arterial structure, mechanics, and repair following endovascular stenting in mice. *Circ. Res.* **104,** 380–387

Loss of Syndecan-1 Induces a Pro-inflammatory Phenotype in Endothelial Cells with a Dysregulated Response to Atheroprotective Flow

Peter L. Voyvodic, Daniel Min, Robert Liu, Evan Williams, Vipul Chitalia, Andrew K. Dunn and Aaron B. Baker

J. Biol. Chem. 2014, 289:9547-9559.
doi: 10.1074/jbc.M113.541573 originally published online February 19, 2014